

First observations of $\psi(2S)$ and $\chi_{cJ}(1P)$ decays to four-body final states $h^+h^-K_S^0K_S^0$ [§]

M. Ablikim¹, J. Z. Bai¹, Y. Ban¹⁰, J. G. Bian¹, X. Cai¹, J. F. Chang¹, H. F. Chen¹⁶, H. S. Chen¹, H. X. Chen¹, J. C. Chen¹, Jin Chen¹, Jun Chen⁶, M. L. Chen¹, Y. B. Chen¹, S. P. Chi², Y. P. Chu¹, X. Z. Cui¹, H. L. Dai¹, Y. S. Dai¹⁸, Z. Y. Deng¹, L. Y. Dong¹, S. X. Du¹, Z. Z. Du¹, J. Fang¹, S. S. Fang², C. D. Fu¹, H. Y. Fu¹, C. S. Gao¹, Y. N. Gao¹⁴, M. Y. Gong¹, W. X. Gong¹, S. D. Gu¹, Y. N. Guo¹, Y. Q. Guo¹, Z. J. Guo¹⁵, F. A. Harris¹⁵, K. L. He¹, M. He¹¹, X. He¹, Y. K. Heng¹, H. M. Hu¹, T. Hu¹, G. S. Huang^{1†}, L. Huang⁶, X. P. Huang¹, X. B. Ji¹, Q. Y. Jia¹⁰, C. H. Jiang¹, X. S. Jiang¹, D. P. Jin¹, S. Jin¹, Y. Jin¹, Y. F. Lai¹, F. Li¹, G. Li¹, H. H. Li¹, J. Li¹, Q. J. Li¹, R. B. Li¹, R. Y. Li¹, S. M. Li¹, W. G. Li¹, X. L. Li⁷, X. Q. Li⁹, X. S. Li¹⁴, Y. F. Liang¹³, H. B. Liao⁵, C. X. Liu¹, F. Liu⁵, Fang Liu¹⁶, H. M. Liu¹, J. B. Liu¹, J. P. Liu¹⁷, R. G. Liu¹, Z. A. Liu¹, Z. X. Liu¹, F. Lu¹, G. R. Lu⁴, J. G. Lu¹, C. L. Luo⁸, X. L. Luo¹, F. C. Ma⁷, J. M. Ma¹, L. L. Ma¹¹, Q. M. Ma¹, X. Y. Ma¹, Z. P. Mao¹, X. H. Mo¹, J. Nie¹, Z. D. Nie¹, S. L. Olsen¹⁵, H. P. Peng¹⁶, N. D. Qi¹, C. D. Qian¹², H. Qin⁸, J. F. Qiu¹, Z. Y. Ren¹, G. Rong¹, L. Y. Shan¹, L. Shang¹, D. L. Shen¹, X. Y. Shen¹, H. Y. Sheng¹, F. Shi¹, X. Shi¹⁰, H. S. Sun¹, S. S. Sun¹⁶, Y. Z. Sun¹, Z. J. Sun¹, X. Tang¹, N. Tao¹⁶, Y. R. Tian¹⁴, G. L. Tong¹, G. S. Varner¹⁵, D. Y. Wang¹, J. Z. Wang¹, K. Wang¹⁶, L. Wang¹, L. S. Wang¹, M. Wang¹, P. Wang¹, P. L. Wang¹, S. Z. Wang¹, W. F. Wang¹, Y. F. Wang¹, Zhe Wang¹, Z. Wang¹, Zheng Wang¹, Z. Y. Wang¹, C. L. Wei¹, D. H. Wei³, N. Wu¹, Y. M. Wu¹, X. M. Xia¹, X. X. Xie¹, B. Xin⁷, G. F. Xu¹, H. Xu¹, Y. Xu¹, S. T. Xue¹, M. L. Yan¹⁶, F. Yang⁹, H. X. Yang¹, J. Yang¹⁶, S. D. Yang¹, Y. X. Yang³, M. Ye¹, M. H. Ye², Y. X. Ye¹⁶, L. H. Yi⁶, Z. Y. Yi¹, C. S. Yu¹, G. W. Yu¹, C. Z. Yuan¹, J. M. Yuan¹, Y. Yuan¹, Q. Yue¹, S. L. Zang¹, Yu. Zeng¹, Y. Zeng⁶, B. X. Zhang¹, B. Y. Zhang¹, C. C. Zhang¹, D. H. Zhang¹, H. Y. Zhang¹, J. Zhang¹, J. Y. Zhang¹, J. W. Zhang¹, L. S. Zhang¹, Q. J. Zhang¹, S. Q. Zhang¹, X. M. Zhang¹, X. Y. Zhang¹¹, Y. J. Zhang¹⁰, Y. Y. Zhang¹, Yiyun Zhang¹³, Z. P. Zhang¹⁶, Z. Q. Zhang⁴, D. X. Zhao¹, J. B. Zhao¹, J. W. Zhao¹, M. G. Zhao⁹, P. P. Zhao¹, W. R. Zhao¹, X. J. Zhao¹, Y. B. Zhao¹, Z. G. Zhao^{1*}, H. Q. Zheng¹⁰, J. P. Zheng¹, L. S. Zheng¹, Z. P. Zheng¹, X. C. Zhong¹, B. Q. Zhou¹, G. M. Zhou¹, L. Zhou¹, N. F. Zhou¹, K. J. Zhu¹, Q. M. Zhu¹, Y. C. Zhu¹, Y. S. Zhu¹, Yingchun Zhu¹, Z. A. Zhu¹, B. A. Zhuang¹, B. S. Zou¹.

(BES Collaboration)

¹ Institute of High Energy Physics, Beijing 100039, People's Republic of China

² China Center for Advanced Science and Technology(CCAST), Beijing 100080, People's Republic of China

³ Guangxi Normal University, Guilin 541004, People's Republic of China

⁴ Henan Normal University, Xinxiang 453002, People's Republic of China

⁵ Huazhong Normal University, Wuhan 430079, People's Republic of China

⁶ Hunan University, Changsha 410082, People's Republic of China

⁷ Liaoning University, Shenyang 110036, People's Republic of China

⁸ Nanjing Normal University, Nanjing 210097, People's Republic of China

⁹ Nankai University, Tianjin 300071, People's Republic of China

¹⁰ Peking University, Beijing 100871, People's Republic of China

¹¹ Shandong University, Jinan 250100, People's Republic of China

¹² Shanghai Jiaotong University, Shanghai 200030, People's Republic of China

¹³ Sichuan University, Chengdu 610064, People's Republic of China

¹⁴ Tsinghua University, Beijing 100084, People's Republic of China

¹⁵ University of Hawaii, Honolulu, Hawaii 96822

¹⁶ University of Science and Technology of China, Hefei 230026, People's Republic of China

¹⁷ Wuhan University, Wuhan 430072, People's Republic of China

¹⁸ Zhejiang University, Hangzhou 310028, People's Republic of China

* Visiting professor to University of Michigan, Ann Arbor, Michigan 48109, USA

† Current address: Purdue University, West Lafayette, Indiana 47907, USA.

First observations of χ_{c0} , χ_{c1} , and χ_{c2} decays to $\pi^+\pi^-K_S^0K_S^0$ and $K^+K^-K_S^0K_S^0$, as well as $\psi(2S)$ decay to $\pi^+\pi^-K_S^0K_S^0$ are presented. The branching fractions of these decay channels are determined using 14×10^6 $\psi(2S)$ events collected at BESII/BEPC. The branching fractions of $\chi_{c0}, \chi_{c2} \rightarrow K_S^0K_S^0$ are measured with improved statistical precision.

PACS numbers: 13.25.Gv, 12.38.Qk, 14.40.Gx

[§] The h^\pm denote charged pions or kaons.

I. INTRODUCTION

Experimental data on charmonia and their decay properties are essential input to test QCD models and QCD based calculations. The importance of the Color Octet Mechanism(COM) [1] in radiative decays of the Υ [2], J/ψ production in inclusive B decays [3], as well as inclusive decays of P-wave charmonia [4] has been emphasized for many years. Recently, QCD predictions of two-body exclusive decays of P-wave charmonium with the inclusion of the COM have been made [5, 6] and compared to previous measurements [7, 8]. More experimental data of two- and four-body exclusive decays of P-wave charmonia with improved precision are important for further testing this new QCD approach including the effect of the COM.

In this paper, results on $\psi(2S)$ and χ_{cJ} ($J = 0, 1, 2$) two- and four-body hadronic decays with inclusion of a pair of K_S^0 mesons are presented. This analysis is based on 14×10^6 $\psi(2S)$ decays collected with BESII at the BEPC e^+e^- Collider. A sample of 6.42 pb^{-1} data taken at 3.65 GeV is used for continuum background studies.

II. BES DETECTOR

The BESII detector is described elsewhere [9]. Charged particle momenta are determined with a resolution of $\sigma_p/p = 1.78\%\sqrt{1+p^2}$ (p in GeV/c) in a 40-layer main drift chamber (MDC). Particle identification is accomplished using specific ionization (dE/dx) information in the drift chamber and time-of-flight (TOF) information in a barrel-like array of 48 scintillation counters. The dE/dx resolution is $\sigma_{dE/dx} = 8\%$; the TOF resolution is $\sigma_{TOF} = 200 \text{ ps}$ for hadrons. A 12-radiation-length barrel shower counter (BSC) measures energies of photons with a resolution of $\sigma_E/E = 21\%/\sqrt{E}$ (E in GeV).

III. MONTE CARLO SIMULATION

A Geant3 based Monte Carlo, SIMBES [10], which simulates the detector response, including interactions of secondary particles in the detector material, is used to determine detection efficiencies and mass resolutions, as well as to optimize selection criteria and estimate backgrounds. Under the assumption of a pure E1 transition, the distribution of polar angle θ of the photon in $\psi(2S) \rightarrow \gamma\chi_{cJ}$ decays is given by $1 + k \cos^2 \theta$ [11] with $k = 1, -\frac{1}{3}$, and $\frac{1}{13}$ for $J = 0, 1$, and 2, respectively. The angular distributions for K_S^0 mesons from $\chi_{c0,2} \rightarrow K_S^0 K_S^0$ decays are produced according to the model of $\chi_{cJ} \rightarrow M\bar{M}$ [12], where M stands for a 0^- meson. Angular distributions for daughters from other decays are generated isotropically in the center-of-mass system of the $\psi(2S)$ or χ_{cJ} .

IV. DATA ANALYSIS

To be regarded as a good photon, a shower cluster in the BSC must have an energy deposit of more than 50 MeV and at least one hit in the first six layers of the BSC. To remove soft photons emitted by charged particles, the differences of azimuthal angles, $d\phi$, and Z coordinates at the first layer of the BSC, dz , between good photons and each charged track must satisfy either a loose requirement (selection-A: $d\phi > 10^\circ$ or $dz > 0.3 \text{ m}$) or a tight requirement (selection-B: $d\phi > 20^\circ$ or $dz > 1.0 \text{ m}$). Here the Z coordinate is defined to point in the positron direction.

Each charged track is required to have a good helix fit. For final states containing charged kaons, particle identification is required; usable particle identification information in one or both of the MDC (dE/dx) and TOF subsystems is necessary. A particle identification χ^2 is calculated for each track for the pion, kaon or proton hypotheses using this information, and the associated probability $prob$ is determined. A track is identified as a kaon, if the probability of the track being a kaon $prob(K) > 0.01$; otherwise it is regarded as a pion. For final states containing only pions, no particle identification is done and all tracks are assumed to be pions.

Each event is required to contain two K_S^0 mesons. The reconstruction of the decay $K_S^0 \rightarrow \pi^+\pi^-$ and related checks are described in detail elsewhere [13]. A K_S^0 candidate must satisfy $|M_{\pi^+\pi^-} - M_{K_S^0}| < 20 \text{ MeV}$ and have a decay length transverse to the beam axis $R_{xy} > 0.3 \text{ cm}$. The K_S^0 sideband sample, used for background estimation, is selected with one $\pi^+\pi^-$ pair within the K_S^0 mass window and the other pair in the K_S^0 mass sideband region defined by $40 \text{ MeV} < |M_{\pi^+\pi^-} - M_{K_S^0}| < 60 \text{ MeV}$.

Four constraint (4C) kinematic fits are performed on the selected events for the following decay modes : (1) $\psi(2S) \rightarrow \gamma K_S^0 K_S^0$, (2) $\psi(2S) \rightarrow \gamma\pi^+\pi^- K_S^0 K_S^0$, and (3) $\psi(2S) \rightarrow \gamma K^+ K^- K_S^0 K_S^0$. The fits are made to each combination of a good photon and two K_S^0 candidates in an event, the combination with the minimum χ^2_{4C} is selected, and the χ^2_{4C} is required to be less than 35. The associated probability $prob_{4C}$ is calculated.

Background from $\psi(2S) \rightarrow \pi^+\pi^- J/\psi$ decay is removed by calculating the mass recoiling, M_{recoil} , against all pairs of oppositely charged tracks, assuming them to be pions, and requiring $|M_{recoil} - M_{J/\psi}| > 25$ MeV. Background contamination from continuum production is found to be negligible for all decay channels.

An unbinned maximum likelihood method is used in fitting the signal for all decay channels except $\psi(2S) \rightarrow h^+h^-K_S^0K_S^0$. The branching fractions of $\psi(2S) \rightarrow \gamma\chi_{cJ}$ ($J = 0, 1, 2$) needed in the measurement are taken from Particle Data Group (PDG) tables [8].

A. $\psi(2S) \rightarrow \gamma K_S^0 K_S^0$

The decay $\psi(2S) \rightarrow \gamma K_S^0 K_S^0$ has one photon plus a pair of K_S^0 candidates. The event should have four charged tracks with total charge zero. The loose photon selection, selection-A, is applied because of the low background in the channel. The $K_S^0 K_S^0$ invariant mass distribution of the selected events is shown in Fig. 1. A few K_S^0 sideband events survive the selection, which is consistent with the low background observed in Fig. 1 (a). No background is expected from $\psi(2S) \rightarrow \gamma\chi_{cJ}$ with $\chi_{cJ} \rightarrow 2(\pi^+\pi^-)$ for $J = 0, 1, 2$ and $\psi(2S) \rightarrow \gamma\chi_{c1}$ with $\chi_{c1} \rightarrow K_S^0 K^\pm \pi^\mp$ according to the analysis of simulated MC events.

The $K_S^0 K_S^0$ invariant mass distribution is fitted with two Breit-Wigner resonances for χ_{c0} and χ_{c2} , each convoluted with Gaussian resolution functions, plus a second order polynomial background. The $\chi_{c0,2}$ widths in the fitting are fixed to their PDG values [8]. The resulting fit is shown in Fig. 1 (b). Including the χ_{c1} resonance in the fit yields zero events for the CP violating decay $\chi_{c1} \rightarrow K_S^0 K_S^0$.

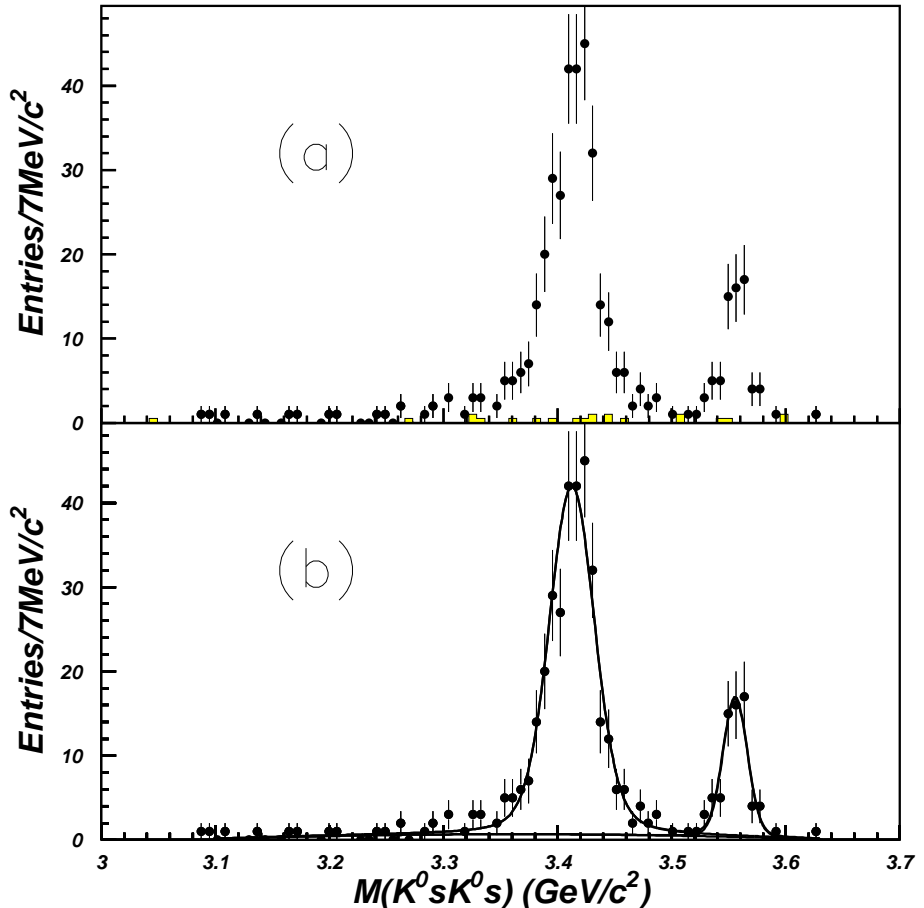


FIG. 1: Distribution of $K_S^0 K_S^0$ invariant mass of $\psi(2S) \rightarrow \gamma K_S^0 K_S^0$ candidates. (a) Points with error bars is for signal events, and histogram is for sideband. (b) Points with error bars is for signal events, and the solid line is the fit described in the text.

B. $\psi(2S) \rightarrow \gamma\pi^+\pi^-K_S^0K_S^0$

The $\psi(2S) \rightarrow \gamma\pi^+\pi^-K_S^0K_S^0$ decay channel contains one photon and six charged tracks with total charge zero. The requirements here are similar to the previous case, but there are two additional pions. Background from π/K misidentification is suppressed by the requirement $prob_{4C}(\gamma\pi^+\pi^-K_S^0K_S^0) > prob_{4C}(\gamma K^+K^-K_S^0K_S^0)$. The $\pi^+\pi^-K_S^0K_S^0$ invariant mass distribution for selected events is shown in Fig. 2.

In Fig. 2 there are two kinds of background in the mass region between 3.0 and 3.64 GeV/c^2 : (1) background corresponding to K_S^0 sidebands, and (2) $\psi(2S)$ decays and χ_{cJ} decays different from the signal channel, where the decays also include a pair of K_S^0 mesons. Studies with K_S^0 sideband events for both data and MC show that K_S^0 sideband background from wrong combinations of $\pi^+\pi^-$ is slightly enhanced in the χ_{cJ} signal region. MC studies show that the smooth background spread over the whole mass region from (2) results mainly from the following decay channels: (a) $\psi(2S) \rightarrow \gamma\chi_{cJ}$ with $\chi_{cJ} \rightarrow 3(\pi^+\pi^-)$ and $\chi_{cJ} \rightarrow K^+K^-K_S^0K_S^0$, (b) $\psi(2S) \rightarrow \pi^0\pi^+\pi^-K_S^0K_S^0$, and (c) $\psi(2S) \rightarrow \omega K_S^0K_S^0$ with $\omega \rightarrow \pi^+\pi^-\pi^0$. Background events in the high mass region above 3.64 GeV/c^2 in Fig. 2 are from $\psi(2S) \rightarrow \pi^+\pi^-K_S^0K_S^0$ decays combined with an unassociated low energy photon.

The $\pi^+\pi^-K_S^0K_S^0$ invariant mass distribution between 3.0 to 3.64 GeV/c^2 is fitted with three Breit-Wigner resonances χ_{cJ} ($J = 0, 1, 2$), convoluted with Gaussian resolution functions, plus a 2nd order background polynomial. The widths of $\chi_{c0,1,2}$ resonances in the fit are fixed to the PDG values. The fit is shown in Fig. 2. The signal area determined from the fit includes signal and K_S^0 sidebands background, which is enhanced in the signal region. The K_S^0 sideband sample in the data is fitted with a fake signal shape, found by fitting K_S^0 sideband sample of signal MC, plus a 2nd order background polynomial. Number of the fake signal events from K_S^0 sideband data is then subtracted from the number of signal events in the result.

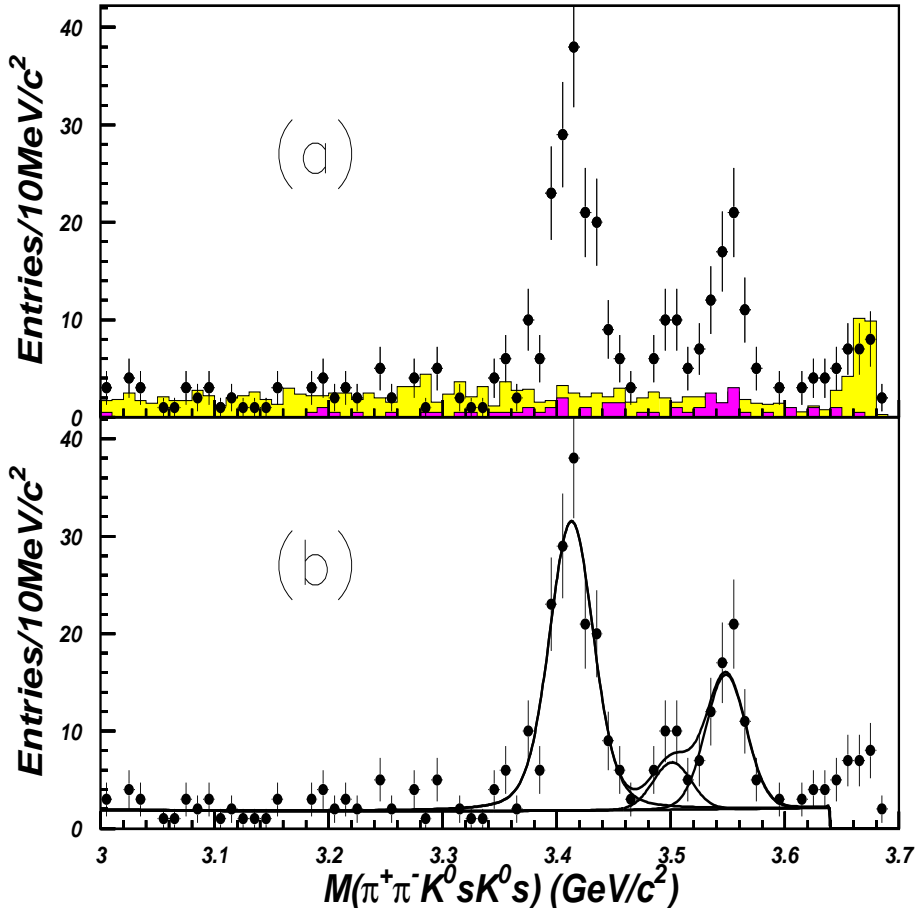


FIG. 2: Distribution of $\pi^+\pi^-K_S^0K_S^0$ invariant mass for $\psi(2S) \rightarrow \gamma\pi^+\pi^-K_S^0K_S^0$ candidates. Points with error bars are the data. The light shaded area in (a) is for background simulation, where some unknown branching ratios are normalized to the background level of χ_{cJ} , and the dark shaded area is for K_S^0 sideband events. The solid line in (b) is the fit.

C. $\psi(2S) \rightarrow \gamma K^+ K^- K_S^0 K_S^0$

The $\psi(2S) \rightarrow \gamma K^+ K^- K_S^0 K_S^0$ decay has the same topology as $\psi(2S) \rightarrow \gamma \pi^+ \pi^- K_S^0 K_S^0$, and thus it is subject to similar event selection criteria except for the kaon identification requirement for two of the charged tracks. First, the $K_S^0 K_S^0$ pair is searched for under the assumption that all charged tracks are pions. Kaon identification is only done for the two charged tracks remaining after reconstruction of the $K_S^0 K_S^0$ pair. We also require $prob_{4C}(\gamma K^+ K^- K_S^0 K_S^0) > prob_{4C}(\gamma \pi^+ \pi^- K_S^0 K_S^0)$ for the 4C kinematic fit probabilities to suppress contamination from $\psi(2S) \rightarrow \gamma \pi^+ \pi^- K_S^0 K_S^0$ decays. The $K^+ K^- K_S^0 K_S^0$ invariant mass distribution for selected events is shown in Fig. 3.

As seen from Fig. 3 only one event survives from the K_S^0 sideband sample for data. MC events for the following possible background channels are generated: (1) $\psi(2S) \rightarrow \gamma \chi_{cJ}$ with $\chi_{cJ} \rightarrow 3(\pi^+ \pi^-)$ and $\pi^+ \pi^- K_S^0 K_S^0$, (2) $\psi(2S) \rightarrow \pi^+ \pi^- K_S^0 K_S^0$, and (3) $\psi(2S) \rightarrow \omega K_S^0 K_S^0$ with $\omega \rightarrow \pi^+ \pi^- \pi^0$. However, no event from these background channels is selected. Another study with a large sample of simulated $\psi(2S) \rightarrow \text{anything}$ [14] shows that negligible background comes from decays of $\psi(2S) \rightarrow \phi K^{*0} K^0 \rightarrow \pi^0 K^+ K^- K_S^0 K_S^0$.

The $K^+ K^- K_S^0 K_S^0$ invariant mass distribution is fitted with three Breit-Wigner resonances, χ_{cJ} ($J = 0, 1, 2$), convoluted with Gaussian resolution functions, plus a flat background. Because of low statistics in the signal region, not only the widths and mass resolutions for the χ_{cJ} ($J = 0, 1, 2$), but also the masses of the χ_{c1} and χ_{c2} in the fitting are fixed to their PDG values. The fitting results are shown in the Fig. 3.

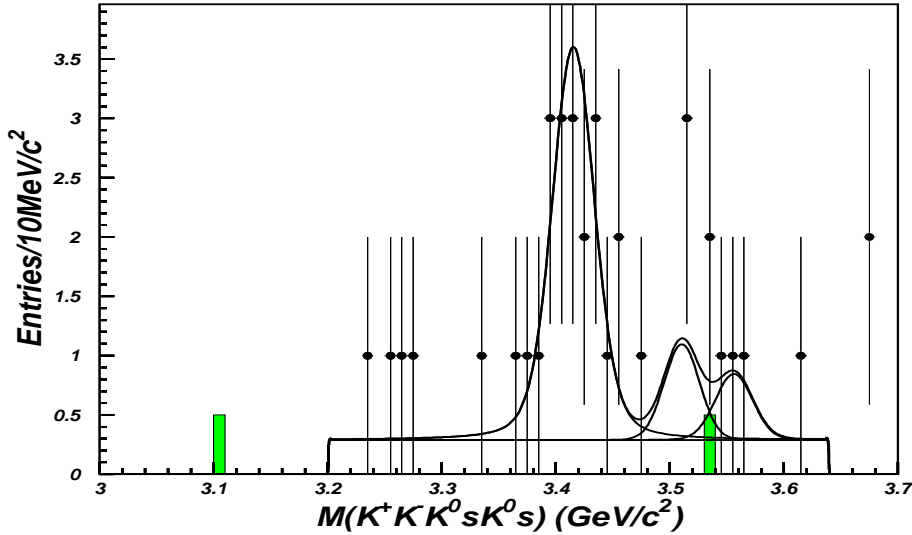


FIG. 3: Distribution of $K^+ K^- K_S^0 K_S^0$ invariant mass of $\psi(2S) \rightarrow \gamma K^+ K^- K_S^0 K_S^0$ candidates. Points with error bars are data. Histogram is for sideband check. The solid line is the fit.

D. $\psi(2S) \rightarrow h^+ h^- K_S^0 K_S^0$

The selection of $\psi(2S) \rightarrow h^+ h^- K_S^0 K_S^0$ decays requires six charged tracks with total charge zero and no good photon in the event, as defined above. Good photons are rejected with the tight selection, selection-B, in order to gain higher detection efficiency for signal events. The K_S^0 reconstruction uses all combinations of oppositely charged tracks assuming all tracks are pions. To further suppress background of $\psi(2S)$ radiative decays, a requirement on the missing momentum of six charged tracks is employed: $P_{miss} < 80$ MeV. The two charged tracks h^+ and h^- recoiling against the K_S^0 pair are assumed to have the same mass m . Using energy-momentum conservation, the mass squared m^2 is calculated from

$$m^2 = \frac{E^4 + (P_{h^+}^2 - P_{h^-}^2)^2 - 2E^2(P_{h^+}^2 + P_{h^-}^2)}{4E^2} \quad (1)$$

where $E = M_{\psi(2S)} - E_{K_S^0 K_S^0}$, and P_{h^\pm} is the momentum of h^+ or h^- . The distribution of m^2 for selected events is shown in Fig. 4. The peak at low mass is consistent with $\pi^+ \pi^-$; there is no evidence for $K^+ K^-$.

Two events from the continuum data sample survive the above selection and their effect will be included in the systematic error. No background is found in MC studies of the following decay channels : (1) $\psi(2S) \rightarrow \gamma \chi_{cJ}$

with $\chi_{cJ} \rightarrow 3(\pi^+\pi^-)$, $\pi^+\pi^-K_S^0K_S^0$, and $K^+K^-K_S^0K_S^0$ and (2) $\psi(2S) \rightarrow \omega K_S^0K_S^0$ with $\omega \rightarrow \pi^+\pi^-\pi^0$. Background estimated using the K_S^0 sideband data is subtracted from the observed number of signal events. A MC study shows that the shape of the charged pion signal in the m^2 spectrum is well described by a Gaussian function, and its mean and resolution are consistent with data. The spectrum is fitted with a Gaussian signal function and a flat background using a binned maximum likelihood fit where the resolution is fixed to the MC determined value. The fitting result is shown in the Fig. 4.

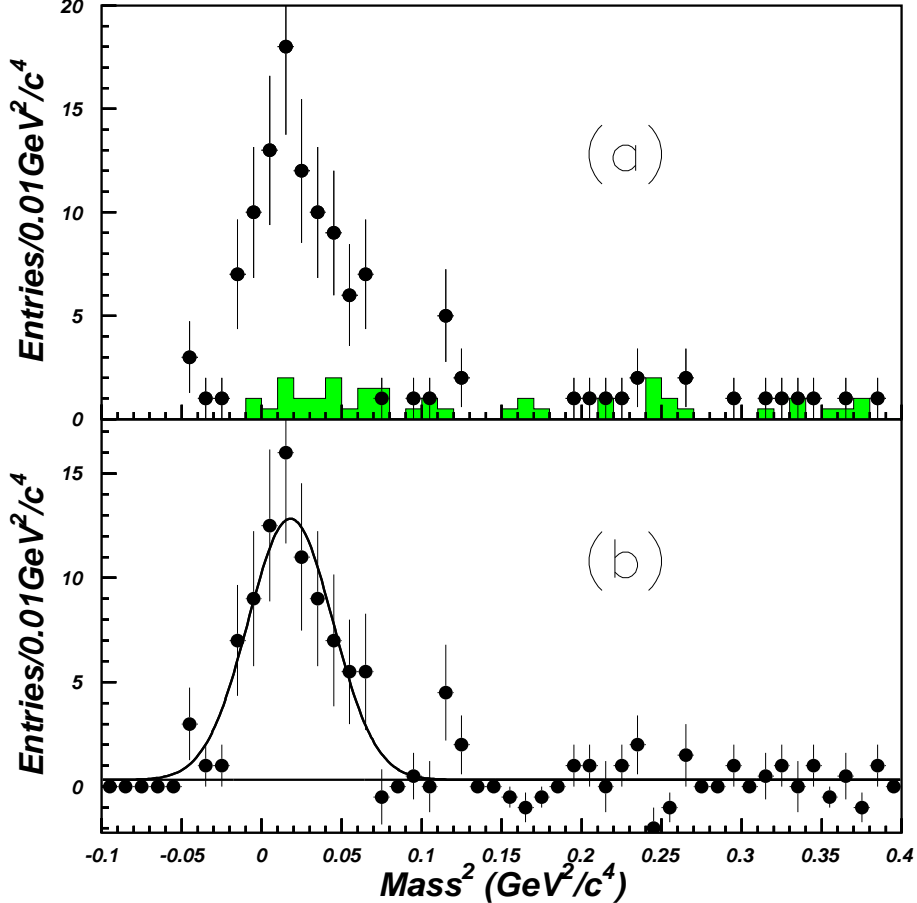


FIG. 4: Distribution of invariant mass squared of the two remaining charged particles after $K_S^0K_S^0$ selection for $\psi(2S) \rightarrow h^+h^-K_S^0K_S^0$. (a) Points with error bars are data. The histogram is the K_S^0 sideband background. (b) Points with error bars are the data with the K_S^0 sideband background subtracted. The solid line is the fit.

E. Systematic Errors

Systematic errors for the efficiency are caused by differences between data and MC simulation. Our studies have determined these errors to be 2% per track for the tracking efficiency, 2% for photon identification, 5% for the 4C kinematic fit, and 2.1% for the K_S^0 reconstruction efficiency. A correction factor due to the overestimate of the K_S^0 reconstruction efficiency of the MC relative to data is determined to be 95.8%. The change of fitting range and background shape function contributes a difference of final results less than 3%. Other systematic errors arise from the uncertainties in the total number of $\psi(2S)$ events, $(14.00 \pm 0.56) \times 10^6$ [15], and in the branching fractions for $K_S^0 \rightarrow \pi^+\pi^-$ and $\psi(2S) \rightarrow \gamma\chi_{cJ}$ ($J=0,1,2$). In $\psi(2S) \rightarrow \pi^+\pi^-K_S^0K_S^0$ decay, with 2 events found in continuum data, an additional error of 7.7% is added.

TABLE I: Summary of the fitting results. Errors for the signal yield n_s , background n_b , mass M , and mass squared m^2 are statistical. The first and second errors for the branching fractions BR are statistical and systematic, respectively. The detection efficiency ϵ and resolution σ for each decay channel from MC, as well as previous branching fractions results, are also shown.

Channel	n_s	n_b	$M_{\chi_{cJ}}$ (MeV/c^2)	ϵ (%)	σ (MeV/c^2)	BR_{meas} (10^{-4})	$UL(10^{-4})$ (CL=90%)	$BR_{PDG}[8]$ (10^{-4})
$\chi_{c0} \rightarrow K_S^0 K_S^0$	322 ± 20		3413.1 ± 1.2	7.96	13.3	$35.1 \pm 2.2 \pm 4.7$	< 0.8	21 ± 6
$\chi_{c1} \rightarrow K_S^0 K_S^0$	0	6.4 ± 2.6	fixed	8.50	12.8			-
$\chi_{c2} \rightarrow K_S^0 K_S^0$	65.1 ± 8.7		3555.7 ± 1.8	8.48	11.8	$8.9 \pm 1.2 \pm 1.3$		7.2 ± 2.7
$\chi_{c0} \rightarrow \pi^+ \pi^- K_S^0 K_S^0$	152 ± 14		3412.9 ± 2.0	2.03	16.8	$65 \pm 6 \pm 10$		-
$\chi_{c1} \rightarrow \pi^+ \pi^- K_S^0 K_S^0$	19.8 ± 7.7		3501.1 ± 6.2	2.20	16.4	$8.0 \pm 3.1 \pm 1.4$		-
$\chi_{c2} \rightarrow \pi^+ \pi^- K_S^0 K_S^0$	57 ± 11		3548.2 ± 3.1	2.04	17.2	$32.4 \pm 6.1 \pm 5.5$		-
$\chi_{c0} \rightarrow K^+ K^- K_S^0 K_S^0$	16.8 ± 4.8		3415.4 ± 6.1	0.91	16.1	$16.0 \pm 4.6 \pm 2.9$		-
$\chi_{c1} \rightarrow K^+ K^- K_S^0 K_S^0$	3.2 ± 2.4	1.8 ± 0.8	fixed	1.12	15.3	$2.5 \pm 1.9 \pm 0.5$	< 5.1	-
$\chi_{c2} \rightarrow K^+ K^- K_S^0 K_S^0$	2.3 ± 2.2	1.8 ± 0.8	fixed	1.05	15.9	$2.6 \pm 2.4 \pm 0.5$	< 5.5	-
Channel	n_s	n_b	$m^2(10^{-3})$ (GeV^2/c^4)	ϵ (%)	$\sigma(10^{-3})$ (GeV^2/c^4)	BR_{meas} (10^{-4})		$BR_{PDG}[8]$ (10^{-4})
$\psi(2S) \rightarrow \pi^+ \pi^- K_S^0 K_S^0$	83.2 ± 9.4		18.0 ± 3.1	2.82	26.5	$2.20 \pm 0.25 \pm 0.33$		-

F. Result and Discussion

Final results of signal yield and branching fractions for the $\chi_{cJ}(1P)$ and $\psi(2S)$ two- and four-body hadronic decays involving K_S^0 pair production are summarized in Table I. The masses of the χ_{cJ} ($J=0,1,2$) extracted from the fits are also listed. The 90% CL upper limits on the branching fractions in the table are obtained using the Feldman-Cousins method [16]. The branching fractions of χ_{cJ} ($J=0,1,2$) decays to $\pi^+ \pi^- K_S^0 K_S^0$ and $K^+ K^- K_S^0 K_S^0$, as well $\psi(2S)$ decay to $\pi^+ \pi^- K_S^0 K_S^0$ are observed for the first time. The branching fractions of χ_{c0} and χ_{c2} decays to $K_S^0 K_S^0$ are measured with improved precision.

Decay rates, determined using updated χ_{cJ} total widths [8] and branching fractions for $\chi_{cJ} \rightarrow \pi^0 \pi^0$, $\pi^+ \pi^-$ ($J = 0, 2$) and $\chi_{cJ} \rightarrow p\bar{p}$ ($J = 1, 2$) decays [8], provide support for the COM (see Table II). According to isospin symmetry, the $\chi_{cJ} \rightarrow K^0 \bar{K}^0$ and $K^+ K^-$ decays should have the same partial width. Assuming equal decay widths for $\chi_{cJ} \rightarrow K_S^0 K_S^0$ and $K_L^0 K_L^0$, we find that the partial width of the $\chi_{c0} \rightarrow K^0 \bar{K}^0$ decay estimated using the result obtained in this paper is not consistent (2.7σ) with the COM prediction for $\chi_{c0} \rightarrow K^+ K^-$, while agreement between them for the corresponding χ_{c2} decays is within 1.1σ . A comparison for the $\chi_{cJ} \rightarrow K^+ K^-$ ($J = 0, 2$) decays shows that the discrepancy between PDG values and the COM predictions is 2.2σ and 1.9σ for χ_{c0} and χ_{c2} states.

Furthermore, the sum of all known χ_{c0} two-body branching fractions is less than 2%. It therefore is important to not only measure more χ_{cJ} decay modes, including many-body modes, but also to determine the COM contribution for the χ_{cJ} many-body decays because of their large portion to the hadronic decay width. Theoretical predictions with inclusion of the COM for χ_{cJ} decays to many-body final states are required for comparison with data.

Acknowledgments

The BES collaboration thanks the staff of BEPC for their hard efforts and the members of IHEP computing center for their helpful assistance, and also K. T. Chao and J. X. Wang for helpful discussions on the COM. This work is supported in part by the National Natural Science Foundation of China under contracts Nos. 19991480, 10225524, 10225525, the Chinese Academy of Sciences under contract No. KJ 95T-03, the 100 Talents Program of CAS under Contract Nos. U-11, U-24, U-25, and the Knowledge Innovation Project of CAS under Contract Nos. U-602, U-34(IHEP); by the National Natural Science Foundation of China under Contract No. 10175060(USTC), and No. 10225522(Tsinghua University); and by the Department of Energy under Contract No. DE-FG02-04ER41291 (U Hawaii).

[1] G.T. Bodwin, E. Braaten and G.P. Lepage, Phys. Rev. D46, 1914(1992); Phys. Rev. D51, 1125(1995);
[2] F. Maltoni and A. Petrelli, Phys. Rev. D59, 074006(1999);
[3] M. Beneke, F. Maltoni and I.Z. Rothstein, Phys. Rev. D59, 054003(1999);
[4] H.W. Huang and K.T. Chao, Phys. Rev. D54, 6850(1996); A. Petrelli, Phys. Lett. B380, 159(1996).
[5] J. Bolz, P. Kroll and G.A. Schuler, Eur. Phys. J. C2, 705(1998); Phys. Lett. B392, 198(1997).

TABLE II: Comparison of partial widths for $\chi_{cJ} \rightarrow \pi\pi, K\bar{K}$ and $p\bar{p}$ decays between PDG [8] and the COM predictions. Also shown is the result based on this analysis.

Decay	$\Gamma_i(PDG)$ in KeV/c^2	$\Gamma_i(COM)$ in KeV/c^2
$\chi_{c0} \rightarrow \pi^+ \pi^-$	49.5 ± 6.7	45.4 [5]
$\chi_{c2} \rightarrow \pi^+ \pi^-$	3.73 ± 0.64	3.64 [5]
$\chi_{c0} \rightarrow \pi^0 \pi^0$	25.3 ± 3.3	23.5 [5]
$\chi_{c2} \rightarrow \pi^0 \pi^0$	2.3 ± 1.5	1.93 [5]
$\chi_{c1} \rightarrow p\bar{p}$	0.066 ± 0.015	0.05627 [6]
$\chi_{c2} \rightarrow p\bar{p}$	0.143 ± 0.018	0.15419 [6]
$\chi_{c0} \rightarrow K^+ K^-$	61 ± 10	38.6 [5]
$\chi_{c2} \rightarrow K^+ K^-$	1.98 ± 0.47	2.89 [5]
$\chi_{c0} \rightarrow K^0 \bar{K}^0$	71 ± 12 (this paper)	
$\chi_{c2} \rightarrow K^0 \bar{K}^0$	3.76 ± 0.80 (this paper)	

- [6] S.M.H. Wong Nucl. Phys. **A674**, 185(2000); Eur. Phys. J. **C14**, 643(2000).
- [7] BES Collab., J.Z. Bai *et al.*, Phys. Rev. D**67**, 032004(2003); Phys. Rev. D**67**, 112001(2003); Phys. Rev. D**60**, 072001(1999); Phys. Rev. Lett., **81**, 3091(1998). CLEO Collab., B.I. Eisenstein *et al.*, Phys. Rev. Lett., **87**, 061801(2001). E835 Collab., M. Andreotti *et al.*, Phys. Rev. Lett., **91**, 091801(2003); S. Bagnasco *et al.*, Phys. Lett. B**533**, 237(2002); M. Ambrogiani *et al.*, Phys. Rev. Lett., **83**, 2902(1999).
- [8] S. Eidelman *et al.* (Particle Data Group), Phys. Lett. B**592**, 1(2004)(URL: <http://pdg.lbl.gov>).
- [9] BES Collab., J.Z. Bai *et al.*, Nucl. Instr. Meth. A**458**, 627 (2001); J.Z. Bai *et al.*, Nucl. Instr. Meth. A**344**, 319 (1994).
- [10] H.M. Liu *et al.*, 'The BESII detector simulation', to be published to NIM.
- [11] G. Karl *et al.*, Phys. Rev. D**13**, 1203(1976); L.S. Brown and R.N. Cahn, Phys. Rev. D**13**, 1195(1976).
- [12] P.K. Kabir and A.J.G. Itey, Phys. Rev. D**13**, 3161(1976).
- [13] Zhe Wang *et al.*, HEP&NP, **27**, 1 (2003).
- [14] J.C. Chen, Phys. Rev. D**62**, 034003(2000).
- [15] X.H Mo *et al.*, HEP&NP, **28** (2004) 455, hep-ex/0407055.
- [16] G. Feldman and R. Cousins, Phys. Rev. D**57**, 3873(1998); J. Conrad, *et al.*, Phys. Rev. D**67**, 012002(2003).